JOURNAL OF COMPUTATIONAL PHYSICS **136,** 263–271 (1997)
ARTICLE NO. CP975707

Numerical Considerations in the Computation of the Electrostatic Free Energy of Interaction within the Poisson–Boltzmann Theory

Alexandru M. Micu,*,† Babak Bagheri,† Andrew V. Ilin,† L. Ridgway Scott,†,‡ and B. Montgomery Pettitt*,†

Department of Chemistry, †Texas Center for Advanced Molecular Computation, ‡Department of Mathematics, University of Houston, Houston, Texas 77204

Received August 13, 1996; revised March 18, 1997

We evaluate two different ways of calculating the contribution of the electrostatic stress to the free energy integral based on Sharp and Hönig's method within the finite difference nonlinear Poisson–Boltzmann equation method with the University of Houston Brownian Dynamics program. We show that only one of these approaches gives consistent results in the limit of zero ionic concentration for interactions of the order of magnitude of the hydrogen bond. The results are compared with results from both the linear Poisson–Boltzmann equation and the Debye–Hückel theory, for ion concentrations within the limits of validity of these approximate methods. We demonstrate this by application to DNA molecules.

1. INTRODUCTION

The nonlinear Poisson–Boltzmann equation (NLPBE) [1] can be derived from the minimization of an ansatz functional. Reiner and Radke proposed that this functional represents the electrostatic free energy and applied it in the study of a system of interacting double layers [2]. Independently, Sharp and Hönig used the variational method to calculate the electrostatic energy of a biomolecule in a continuum solvent of specified dielectric behavior [3]. Numerical agreement between their method and the charging integral method has been shown by Sharp and Hönig [3]. Recently, Zhou has given an analytical proof of the equivalence of Sharp's energy-density integral and the charging integral [4]. The former is much more efficient to evaluate. We demonstrate here that there are two different ways of computing the energy-density integral, one of which appears to be more accurate for grid sizes typically used.

Due to recent improvements in numerical algorithms and computer performance, Poisson–Boltzmann theories and their finite-difference implementations have become widely used in computational biophysics and computational biochemistry. The main advantage of these methods resides in their speed, whereas the more detailed and arguably more accurate perturbation methods, which make use of explicit solvents, require lengthy molecular dynamics simulations or solutions to nonlinear integral equations [5].

Recent applications of the Poisson–Boltzmann theory include computations of electrostatic forces on solvated molecules [8], solvation energies for charged rods in the presence of salt [9], solvation of vesicles of ionic amphiphiles [10], interaction energies and forces for colloidal particles [11, 12], membrane-electrolyte systems [13] and numerous others. It has been considered a reference for other approximate methods [14, 15] and has been parameterized to give results in qualitative agreement with experimental quantities for a range of compounds while the free-energy perturbation technique has proven to be both more costly and problematic [16], although potentially exact. Comparisons with grand canonical Monte Carlo methods and the hyper-netted chain formalism have shown that PBE retains its semiquantitative utility even in the range of moderate to high concentrations of bulk salt [17].

In this paper, we focus on the calculation of the approximate electrostatic free energy of interaction (EFEI) arising from hydrogen bonds between DNA strands. Indeed, it is well known that the specific base pairing in nucleic acids is a consequence of recognition through hydrogen bonds. While single strands can adopt a helical conformation in saline solution due to stacking effects among adjacent bases, hydrogen bonds are responsible for the specificity and impart the stability of the double helix through the correct pairing of the bases. The hydrogen bond can be represented in a classical force field as a combination of electrostatic and van der Waals forces.

While thermodynamic perturbation theory methods with a fully atomic representation of the solvent require extensive and costly simulations, the Poisson–Boltzmann methods present an inexpensive qualitative method of evaluating the approximate EFEI ($\Delta G(\phi)$) between DNA strands.

The potential biological and medical interest of the work we present here resides in gaining insight about new binding motifs which can be aimed at inhibiting the transcription process [18]. Indeed, much experimental work lately concentrates on therapeutic intervention at the level of the nucleic acid (for reviews in this area of work see [19, 20]).

0021-9991/97 $25.00

Numerous drugs and chemotherapeutics that bind to nucleic acids are already available on the market and research efforts are directed towards the improvement of their affinity for the genetic material [21, 22]. However, none of these drugs show the specificity necessary for targetting a particular gene. The high specificity of base pairing in nucleic acids has led to the idea of engineering a second RNA strand (in translation inhibition) or a third DNA strand (transcription inhibition) that would specifically bind to a segment of the target mRNA or DNA. To ensure specificity in the context of the size of the human genome these complementary strands should be at least 17 base-pairs long [23]. The average ΔG^{el} per base pair in a double stranded DNA is around 0.6–0.7 kcal/mol/base pair for a typical T · A pair [24]. It is therefore important to assess the accuracy of energy evaluations when using finite difference NLPBE to investigate interactions with this magnitude. In biological environments, these energies are of the order of $k_b T$, where k_b is Boltzmann constant and T is the temperature.

This paper is organized as follows. We give the theoretical basis for our numerical arguments, then in a first example of calculation we try to determine whether a finite difference method applied to the Poisson–Boltzmann equation gives reliable results in the limit of zero ionic concentration for a very simple system and how the grid spacing and grid size affect the results. We next compare the finite difference PBE results to calculations within the Debye–Hückel asymptotic limit. Indeed, the Debye–Hückel theory is known for giving exact results in the limit of infinite dilution. Since the Debye–Hückel theory can be derived from the Poisson–Boltzmann theory, the results should differ only by numerical errors. A third example will show how the FDPBE performs on more complex, highly charged molecules such as duplex DNA. We will show how the two numerical methods compare and how they compare to experimental data with established parameters.

2. METHODS

In the following we present general aspects of the discretization methods applied to the NLPBE and two ways the electrostatic free energy can be integrated.

2.1. *A Model Problem and Its Variational Formulation*

We consider a scalar nonlinear elliptic 3D problem of the form

$$\begin{aligned} -\sum_{i=1}^{3} \frac{\partial}{\partial x_i}\left(\varepsilon(x)\frac{\partial \phi}{\partial x_i}\right) + N(\phi) &= \rho(x), \quad x \in \Omega, \\ \phi &= \phi_0(x), \quad x \in \partial\Omega, \end{aligned} \tag{1}$$

where ε, N, ρ, and ϕ_0 are given functions.

For Eq. (1) to be elliptic [25], the function $\varepsilon(x)$ needs to be greater than a fixed positive constant at almost every point x, as well as essentially bounded. However, there is no need for $\varepsilon(x)$ to be continuous, and in many important physical applications it is not. We also assume that the function ϕ_0 can be extended to all of the domain as a function with square-integrable gradient, i.e., as a member of the Sobolev space $H^1(\Omega)$ [25]. We assume that the nonlinear function $N(\phi)$ is the derivative of a function $M(\phi) \in C^2(R^1)$: $N(\phi) = \partial M(\phi)/\partial\phi$.

A finite difference treatment of the problem in Eq. (1) for an arbitrary geometry can be problematic, especially when $\varepsilon(x)$ is discontinuous. However, the variational formulation is quite simple. Define

$$a(\phi, v) := \int_\Omega \sum_{i=1}^{3} \varepsilon(x)\frac{\partial \phi}{\partial x_i}\frac{\partial v}{\partial x_i}\,dx \tag{2}$$

and define the space $V \subset H^1(\Omega)$ of functions v (for which the form $a(v, v)$ is finite) which satisfy the homogeneous essential boundary conditions ($v(x) = 0$, $x \in \partial\Omega$) of the problem on $\partial\Omega$ as described in [25]. Also, we use the standard L^2 inner-product

$$(\omega, v) := \int_\Omega \phi(x)v(x)\,dx. \tag{3}$$

Using these ingredients, Eq. (1) can be posed as follows.

Find $\phi(x)$ such that $\phi(x) - \phi_0(x) \in V$ and

$$a(\phi, v) + (N(\phi), v) = (\rho, v) \quad \forall v \in V. \tag{4}$$

One can show that a solution of Eq. (4) is a solution of the initial problem in Eq. (1), if, e.g., $\phi \in H^2(\Omega)$ [25]. In any case, (4) provides a more general formulation of the equation (1) which allows the definition of solutions of physical interest even when (as will be the case of interest here) ε is discontinuous, and hence not all of derivatives in (1) are defined.

The quantity

$$\Delta G(\phi) = (\rho, \phi) - \frac{1}{2}a(\phi, \phi) - \int_\Omega M(\phi)\,dx \tag{5}$$

is frequently physically meaningful and often related to the energy of the system. One can show that the solution of Eq. (4) minimizes the energy functional (5) in the space of functions $\{\phi: \phi - \phi_0 \in V\}$, i.e., the variation

$$\frac{d}{ds}\Delta G(\phi + sv)\bigg|_{s=0} = 0 \quad \forall v \in V. \tag{6}$$

The energy functional in Eq. (5) can be computed using

the definitions (2) and (3) or, at its minimum, using the defining property (4) for $v = \phi - \phi_0$:

$$a(\phi, \phi) = (\rho, \phi - \phi_0) + a(\phi, \phi_0) - (N(\phi), \phi - \phi_0). \quad (7)$$

Integrating the term $a(\phi, \phi_0)$ by parts and using Eq. (1) we can rewrite

$$a(\phi, \phi) = (\rho, \phi) - (N(\phi), \phi) + \int_{\partial\Omega} \varepsilon(x) \frac{\partial \phi}{\partial n} \phi_0 \, dx, \quad (8)$$

where n is the outward unit normal vector to the boundary $\partial\Omega$. So, the minimal value of the energy functional in Eq. (5) can be evaluated by

$$\Delta G(\phi) = \frac{1}{2}(\rho, \phi) - \int_\Omega M(\phi) \, dx + \frac{1}{2}(N(\phi), \phi) + \frac{1}{2}\int_{\partial\Omega} \varepsilon(x) \frac{\partial \phi}{\partial n} \phi_0 \, dx. \quad (9)$$

That is, we replace the integral $a(\phi, \phi)$, of a derivative quantity involving a coefficient ε with possible discontinuities, by terms which require no derivatives and do not involve ε, except for the boundary integral $\int_{\partial\Omega} \varepsilon(x)(\partial\phi/\partial n)\phi_0 \, dx$. This term is quite small in typical biological applications and, moreover, the boundary can be chosen so that ε and $\partial\phi/\partial n$ are smooth there. The last term can be computed accurately for smooth $\varepsilon(x)$, ϕ_0 and $\partial\phi/\partial n$ on $\partial\Omega$, in contrast with $a(\phi, \phi)$.

2.2. *Discretization of the Model Problem*

The finite element method for approximating Eq. (1) is straightforward to derive once we pick a space $V_h \subset V$ of approximating functions. With this, we define a finite element approximation ϕ_h by adding subscripts h to Eq. (4). Thus we want to find ϕ_h such that $\phi_h - \phi_0 \in V_h$ and

$$a(\phi_h, v) + (N(\phi_h), v) = (\rho, v) \quad \forall v \in V_h. \quad (10)$$

The energy functional $\Delta G(\phi_h)$ can be approximated by the above two approaches. It can be computed using the definitions in Eq. (5):

$$\Delta G(\phi_h) = (\rho, \phi_h) - \frac{1}{2} a(\phi_h, \phi_h) - \int_\Omega M(\phi_h) \, dx, \quad (11)$$

or using the (potentially more accurate) equation (9):

$$\Delta G(\phi_h) = \frac{1}{2}(\rho, \phi_h) - \int_\Omega M(\phi_h) \, dx + \frac{1}{2}(N(\phi_h), \phi_h) + \frac{1}{2}\int_{\partial\Omega} \varepsilon(x) \frac{\partial \phi_h}{\partial n} \phi_0 \, dx. \quad (12)$$

It is interesting to notice that the quantity (ρ, ϕ_h), as well as other terms in Eq. (12) have extra approximation accuracy in comparison with the apparent difference between $a(\phi_h, \phi_h)$ and $a(\phi, \phi)$. For example, if V_h contains piecewise linear functions, then $\|\phi - \phi_h\|_2$ is of order h^2 (if ε is smooth), whereas its derivatives can be no better than order h. Here,

$$\|\psi\|_2 = \left(\int_\Omega \psi(x)^2 \, dx \right)^{1/2} \quad (13)$$

denotes the usual $L^2(\Omega)$ norm for any square-integrable function ψ. Thus,

$$|(\rho, \phi_h) - (\rho, \phi)| \le C_\phi \|\rho\|_2 h^2, \quad (14)$$

assuming ϕ is sufficiently smooth. Similarly, one can show that

$$|(N(\phi_h), \phi_h) - (N(\phi), \phi)| + \left| \int_\Omega M(\phi_h) \, dx - \int_\Omega M(\phi) \, dx \right| \le C_\phi h^2, \quad (15)$$

assuming $M(\phi) \in C^2(\mathbb{R}^1)$.

Since all of these terms are evidently of order h^2, whereas the derivative error is only of order h, it might seem obvious that (12) is more accurate. However, it turns out to be more subtle than that. The same order h^2 estimate for $a(\phi_h, \phi_h) - a(\phi, \phi)$ can be derived as follows. For simplicity, let us assume that $\phi_0 \equiv 0$. Then $\phi_h \in V_h$ and choosing $v = \phi_h$ in (10) shows that (11) and (12) are *identical.* However, the difficulty with (11) is computing the exact integrals when ε is complicated, e.g., discontinuous.

2.3. *Finite Difference Approximation*

In the case that the coefficient $\varepsilon(x)$ is constant and the mesh is regular, Eq. (10) is identical to standard finite difference equations on a seven-point stencil, provided that suitable quadrature is used for the right-hand side. For example, suppose V_h consists of continuous piecewise trilinear functions on a tensor-product mesh in three dimensions, or a corresponding tetrahedral subdivision of such a mesh with continuous piecewise linear functions. Let the L^2 inner-product be approximated by the trapezoidal rule, which we denote by $(\phi, v)_h$. Now let $\phi_h - \phi_0 \in V_h$ be such that

$$a(\phi_h, v) + (N(\phi_h), v)_h = (\rho, v)_h \quad \forall v \in V_h. \quad (16)$$

The variational problem in Eq. (16) is identical to a standard finite difference method [25]. In the case that $\phi_0 \equiv 0$,

$$\begin{aligned}\Delta G(\phi_h) &:= (\rho, \phi_h)_h - \tfrac{1}{2}a(\phi_h, \phi_h) - (1, M(\phi_h))_h \\ &= \tfrac{1}{2}(\rho, \phi_h)_h - (1, M(\phi_h))_h + \tfrac{1}{2}(N(\phi_h), \phi_h)_h,\end{aligned} \tag{17}$$

where "1" denotes the function that is identically one. That is, we are indicating that the same quadrature rule is used to evaluate $\int_\Omega M(\phi_h)\, dx$ as for the inner-products. Thus we conclude that the two methods for computing ΔG are essentially identical for constant $\varepsilon(x)$.

In the case that the coefficient $\varepsilon(x)$ is discontinuous, the finite element solution cannot be computed exactly unless the discontinuities of $\varepsilon(x)$ fall on element boundaries. Similarly, a finite difference approximation will likely no longer satisfy a relationship like Eq. (17). In this case, using expression (9) may be much more accurate as an approximation to $\Delta G(\phi)$ than computing the energy functional directly from Eq. (5).

2.4. *Application to Electrostatic Free Energy Calculations*

Let us present the two different forms of the electrostatic free energy of interaction (EFEI) integral for the nonlinear Poisson–Boltzmann problem. For the sake of clarity we will present the basic physical formulas. A more complete discussion of these equations and their implementation can be found in references [1, 3].

The nonlinear Poisson–Boltzmann equation (NLPBE) can be written in the following nondimensional form for a univalent electrolyte solution:

$$\begin{aligned}-\sum_{i=1}^{3}\frac{\partial}{\partial x_i}\left(\varepsilon(x)\frac{\partial\phi}{\partial x_i}\right) + 2ec^b\sinh\left(\frac{e\phi}{k_bT}\right) &= \rho^f(x), \quad x \in \Omega, \\ \phi &= \phi_0(x), \quad x \in \partial\Omega,\end{aligned} \tag{18}$$

where $\varepsilon(x)$ is the dielectric constant (permittivity), $\rho^f(x)$ is the charge density, c^b is the bulk concentration of ions in the solvent ($c^b = \sum c_i$), k_b is the Boltzmann constant, e is the electron charge constant, T is the temperature, and $\phi(x)$ is the electrostatic potential. Notice that the NLPBE problem (18) can be derived from the model problem (1) by choosing $M(\phi) = 2k_bTc^b \cosh(e\phi/k_bT)$.

The solution of Eq. (18) minimizes the free-energy functional. The energy integral, as used in the standard releases of the popular codes UHBD and Delphi has the form [1, 3]

$$\begin{aligned}\Delta G(\phi) = \int_\Omega \Bigg\{\rho^f(x)\phi - 2K_bTc^b\left[\cosh\left(\frac{\phi e}{k_bT}\right) - 1\right] \\ - \frac{1}{2}\sum_{i=1}^{3}\varepsilon(x)\frac{\partial\phi}{\partial x_i}\frac{\partial\phi}{\partial x_i}\Bigg\}\, dx,\end{aligned} \tag{19}$$

where Ω is the volume over which the integration is carried out. In what follows, we will refer to the above integral as NLPBE1. It clearly is the same as (11) for our model problem.

In the previous subsection we have shown that there are reasons to believe that the finite difference computation of the square gradient is prone to extreme numerical errors. Thus, the second way (9) of computing $\Delta G(\phi)$ may be of significant interest. In this case, it takes the form

$$\begin{aligned}\Delta G(\phi) = \int_\Omega \Bigg\{\frac{\rho^f(x)\phi}{2} - 2k_bTc^b\left[\cosh\left(\frac{\phi e}{k_bT}\right) - 1\right] \\ + \phi ec^b\sinh\left(\frac{\phi e}{k_bT}\right)\Bigg\}\, dx + \frac{1}{2}\int_{\partial\Omega}\varepsilon(x)\frac{\partial\phi}{\partial n}\phi_0\, dx.\end{aligned} \tag{20}$$

In the following we shall refer to the integral in Eq. (20) as NLPBE2.

Equation (20) converges to

$$\Delta G(\phi) = \frac{1}{2}\int_\Omega \rho^f(x)\phi\, dx + \frac{1}{2}\int_{\partial\Omega}\varepsilon(x)\frac{\partial\phi}{\partial n}\phi_0\, dx \tag{21}$$

in the limit $c^b \to 0$. The last integral on the right-hand side of the equation vanishes for large domains. In the following we shall refer to integral in Eq. (21) as LPBE.

3. RESULTS

3.1. *Two Point Charges in a Dielectric Continuum*

We first consider the simplest asymptotic limit. According to Eq. (20), in the limits of zero bulk salt concentration, the energies must be the same, regardless of the method used to derive the potentials (NLPBE or LPBE). When the free energy of interaction for two point charges at a distance d in a continuum dielectric is calculated, in the absence of any mobile ions, the result should trivially equal the value predicted by Coulomb's law,

$$\frac{q_iq_j}{4\pi\varepsilon_0\varepsilon_r d}, \tag{22}$$

where ε_0 and ε_r are the electric permittivity and the relative permittivity, and q_i and q_j are two point charges.

TABLE I

EFEI for Two Point Charges at 4 Å Distance from Each Other in a Continuum of Relative Permittivity $\varepsilon_r = 80$

Method	ΔG^{el} (kcal/mol)
LPBE	1.0383
NLPBE1	1.8328
NLPBE2	1.0383
Coulomb	1.0375

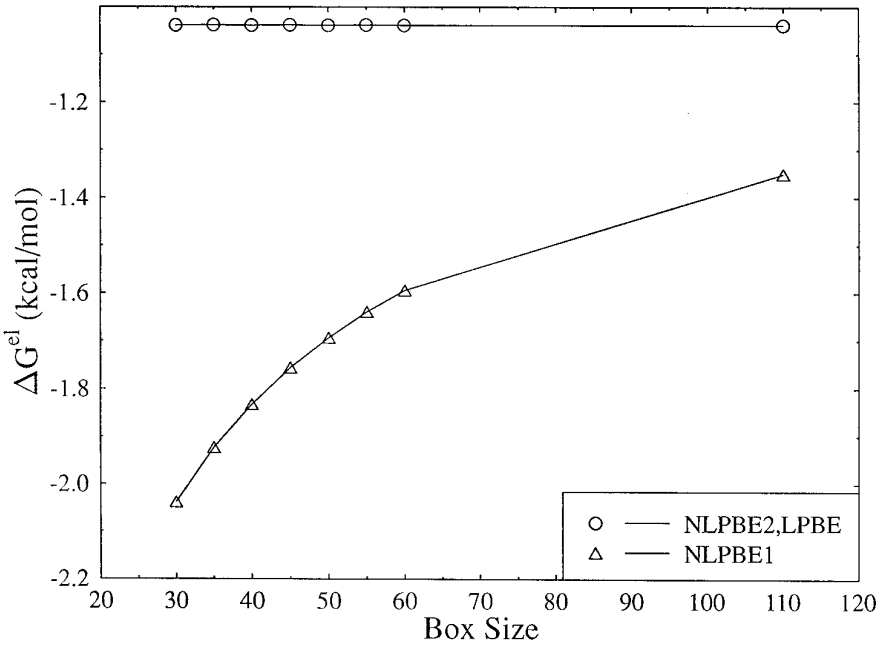

FIG. 1. The electrostatic free energy of interaction as a function of the grid size. The LPBE and NLPBE2 methods provide the same results. NLPBE1 provides results dependent on the grid size.

We considered two point charges at a distance of 4 Å in a continuum dielectric of permittivity $\varepsilon_r = 80$, of relevance to aqueous solutions. The grid spacing was set to 0.2 Å while the cubic grid side's size was varied from 30 to 60 points per side. An additional calculation was run with a 110-point grid size. The boundary potential is calculated as the sum of the potential created by independent DH spheres [7]. The electrostatic interactions are formally long-ranged interactions and the potential will not drop to zero at the box boundaries unless an infinite box size is used or the boundary conditions are set to zero in a finite box. The latter case corresponds to forcing the system's neurality by introducing excess counterions in the box. The results are further affected by the nonlinearity of the system. Our tests have shown (results not given here) that forcing zero boundary conditions leads to results inconsistent with the analytical results.

Table I shows the results as calculated analytically via Coulomb's law, using LPBE and NLPBE, and a grid size of $40 \times 40 \times 40$. In the latter case the free energy was calculated using both integrals NLPBE1 and NLPBE2. To account for numerical errors, the system was translated by 0.01 Å in the x, y, and z directions simultaneously, in 20 successive steps and the results averaged. The results show an error of about 80% when the integration is carried out with NLPBE1, while energies calculated from LPBE and with NLPBE2 are identical. Since the only difference between the two methods consists in the way the integration of the energy is carried out, errors during the nonlinear iterations cannot be the cause.

When the grid spacing is reduced, the agreement between the finite difference method and Coulomb's equation gets better, as expected, and, for a $160 \times 160 \times 160$ box with a 0.05 Å grid spacing, the results are identical up to five significant figures (due to the large amount of memory required this calculation has been done on 32 nodes of a KSR-1).

Figure 1 shows the dependence of the free energy of interaction with the grid size. NLPBE2 and LPBE gave exactly the same results and proved to be very stable within the range of box sizes considered. NLPBE1 results appear to be strongly dependent on the size of the box, which confirms our hypothesis from Section 2, namely, that this way of integration leads to increased numerical errors.

In an attempt to understand the influence of the two methods of summation on the results outside of the limiting case, we have calculated the energies of interaction for concentrations of bulk ions going from 0 to 2000 mM. Figure 2 shows the variation of the EFEI with the ionic strength, as calculated with LPBE, NLPBE1, and NLPBE2. While LPBE and NLPBE2 provide very good agreement with each other at low ionic strengths, at higher concentrations in bulk ions, the two methods diverge. This is a consequence of the higher terms in the development of the charge density (see, for example, [26]) compared to

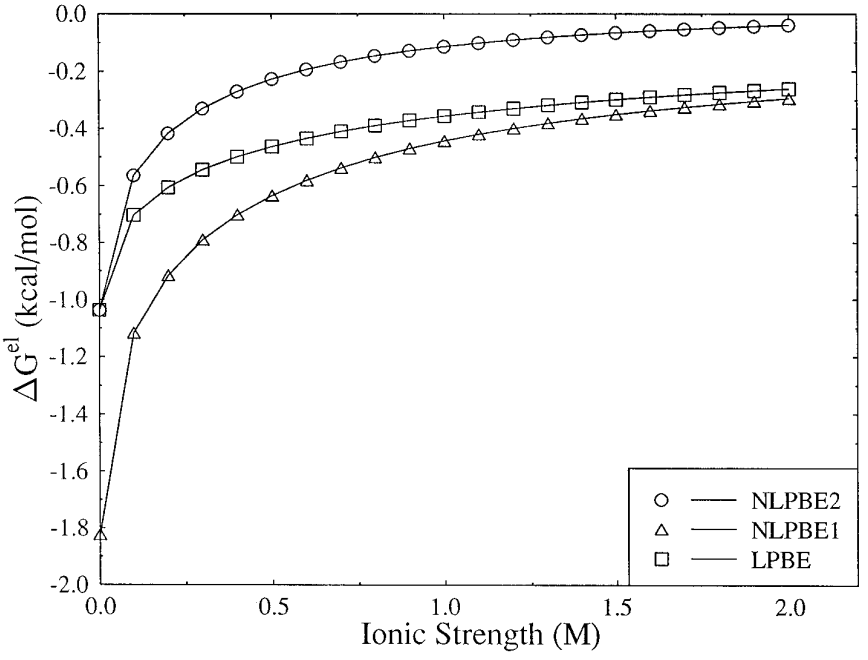

FIG. 2. The electrostatic free energy of interaction as a function of the ionic strength. The concentration in bulk ions was varied from c^b = 0.0 M to 2.0 M.

the linear equation (18). Intuitively, the second method of summation (NLPBE2) provides a better behavior of the curve since we would expect the interaction energies between our particles to vanish at high ionic strengths. However, PB theories are well known to have a number of deficiencies as a theory of ionic solutions due to lack of explicit intramolecular correlations. Our purpose here is simply to consider the numerical aspects.

3.2. *One Sphere in a Continuum Dielectric*

The Debye–Hückel theory provides an asymptotic solution to the problem (18) for a spherical geometry. The results of the Debye–Hückel theory are formally exact in the limit of low concentration and are accepted to be in good agreement with experiments for bulk salt concentrations of less than 5 mM [26]. Table II shows the free energy of solvation for a sphere of radius 2 Å in a continuum dielectric of $\varepsilon_r = 80$ and a concentration of 5 mM as calculated from DH theory, LPBE and NLPBE with the two methods of summation discussed in the previous section. The center of the sphere was translated by 0.01 Å in the x, y, and z directions simultaneously and the results averaged to account for numerical errors. Of course, being derived within the LPBE, the Debye–Hückel theory gives results in good agreement with the first one, the differences possibly being due to numerical imprecisions. This type of calculation is more relevant for the NLPBE methods which, at very small concentrations, should provide results in reasonable agreement with experimental data and, implicitly, with the DH theory.

The second method of summation shows a better agreement with both DH theory and LPBE. For higher concentrations in bulk salt, the lack of analytical results makes it difficult to draw numerical conclusions without resorting to extremely costly explicit simulations.

3.3. *EFEI for Watson–Crick Base Pairs*

The NLPBE has been recently used in a variety of calculations on molecules of biological interest, e.g., computation of electrostatic energies of hydrated molecules [27],

TABLE II

EFEI of Solvation for a Sphere of 2 Å Radius in a Continuum Dielectric of Realtive Permittivity $\varepsilon_r = 80$ and a Bulk Ionic Strength of $c^b = 5$ mM

Method	$\Delta G(\phi)$(kcal/mol)
Debye-Hückel	−0.0456
LPBE	−0.0443
NLPBE1	−0.0904
NLPBE2	−0.0511

Note. The grid spacing was 0.2 Å and the grid size 60 × 60 × 60.

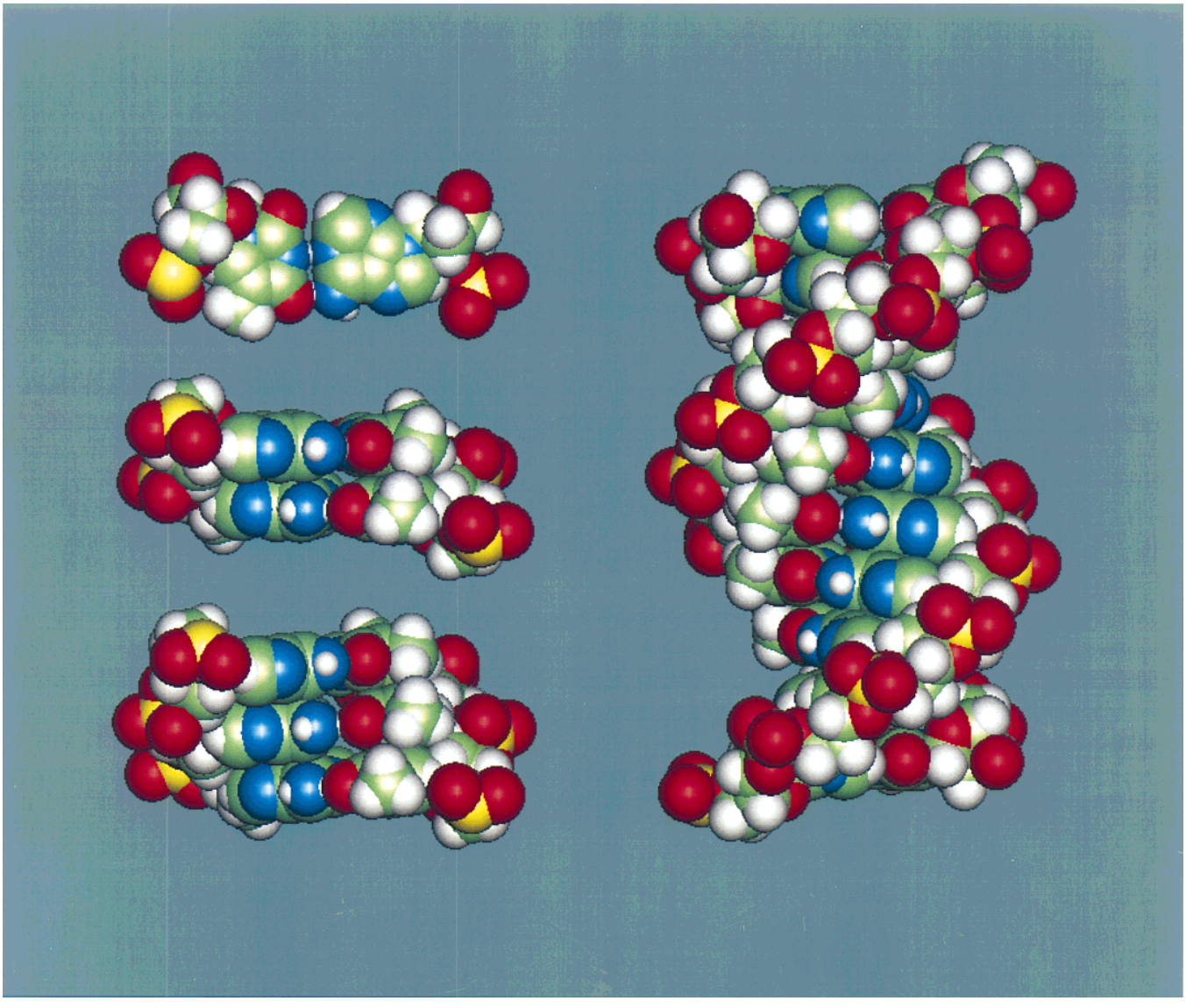

FIG. 3. The four DNA systems (results shown in Table III) with atoms represented as spheres of low dielectric permittivity in a continuum of high dielectric permittivity. From top left, counterclockwise: a T · A base pair viewed from above and side views of two, three, respectively, 10 parallel T · A planes.

interaction energies for protein-DNA complexes [28], solvation free energies [29, 30].

One of the most challenging problems in biophysics consists in understanding the energetics underlying the binding of DNA strands. This would, for instance, permit prediction of binding energies between drugs and the genetic material. It is well known that single DNA strands tend to adopt a stacked conformation in solution. This tendency (due to the hydrophobic nature of the bases) is believed to be at least in part at the origin of the three-dimensional structure of the genetic material. However, the specificity of base pairing is a consequence of the hydrogen bonds established between the bases in different strands and it is widely acknowledged that hydrogen bonds are mostly electrostatic in their nature. It is therefore of interest to be able to precisely and accurately evaluate the EFEI between DNA bases with the PB equation. Direct simulation of free energies would be 10^4–10^5 times more computationally demanding than FDPB.

It is known that the finer the grid spacing, the better the results provided by finite difference methods, until machine precision is reached. This implicitly limits the size of the system to be considered. We will restrict ourselves here to a comparison between the results obtained with LPBE and the two methods of summation from NLPBE for a Watson–Crick T · A base pair. The DNA systems

TABLE III

EFEI in kcal/mol for a Watson–Crick T · A Base Pair in a Continuum Dielectric of Relative Permittivity $\varepsilon_r = 78$ and Ionic Strength $c^b = 0$ mM and $c^b = 200$ mM

System	Method	$c^b = 0$ mM	$c^b = 200$ mM
1-plane	NLPBE1	−1.1692 ± 0.0980	−1.5469 ± 0.0984
	NLPBE2	−1.3388 ± 0.0984	−1.5943 ± 0.0984
2-planes	NLPBE1	−1.1960 ± 0.1466	−2.6777 ± 0.1472
	NLPBE2	−1.8710 ± 0.1470	−2.8603 ± 0.1472
3-planes	NLPBE1	−0.3418 ± 0.2394	−3.7129 ± 0.2403
	NLPBE2	−1.8719 ± 0.2403	−4.1813 ± 0.2403
10-planes	NLPBE1	29.0022 ± 0.4721	−6.0000 ± 0.4585
	NLPBE2	15.6019 ± 0.4510	−12.5920 ± 0.4541
	Expt*		−8.8 ± 0.5

Note. The experimental value for a double stranded T · A decamer is from [24].

(see Fig. 3) were built and oriented into a classic B conformation [31] with the Quanta molecular modeling package [32].

The dielectric permittivity of water was set to 78 while the interior of the molecules had a relative permittivity of 2 to account for the fluctuations of the molecular dipoles. Grid points near the boundary were assigned intermediate values [7, 33]. The atomic charges and Van der Waals radii were those from version 22.0 of CHARMM [32]. The WC base pair was centered in a mesh of $110 \times 110 \times 110$. The grid spacing was set to 0.35 Å. The boundary potentials were calculated as sums of potentials from independent spheres (the flag option 2 within UHBD) [7]. To account for the effects of different relative positions of the molecules with respect to the grid, the WC base pairs were rotated by 80°, in increments of 10°, around each cartesian axis. The average values with the respective variances are given in Table III.

We should emphasize the important differences in energy between the two methods for the systems in a zero ionic strength environment. In particular, the difference between two and three planes breaks the trend and shows considerable discrepancy between the two types of methods. At 200 mM ionic strength, the two methods give closer results. However, when the size of the system (and therefore the charge) is increased, the results of the two methods differ noticeably.

Further work on more sophisticated systems such as triplex DNA and drug-DNA complexes are in progress and should provide us with more insights on the best method to use for biomolecules.

4. DISCUSSION

For accurate calculations with finite difference methods on systems with interaction energies of the order of magnitude of the hydrogen bond, our results suggest that careful consideration should be paid to both the mode of summation and the grid spacing. The only way to assess the correctness of our calculations is to perform calculations in limiting conditions for which analytical asymptotic results are available. For low salt concentrations, the energy integrals corresponding to NLPBE and LPBE should be in reasonable agreement with each other and with the energies calculated within the Debye–Hückel theory. Failure to do so indicates problems in the numerical algorithms or inadequate methods.

The energy integral NLPBE2 seems to produce more reliable results than the corresponding integration for LPBE, when considering hydrated molecules in solutions with a slightly higher concentration of bulk salt (see Fig. 2). However, it is well known that use of the NLPBE at some point contradicts physical laws [26, 35–38] due to the lack of molecular correlations. Our models were within the generally accepted range of applicability of the method.

For larger molecules, such as DNA helices, a quick extrapolation can be made. If we admit that a single DNA strand in its helical form (B or A) can be represented as a cylinder with the given amount of negative charges, the same cylinder can also contain, within a good approximation, both strands (the initial and its complement). The potential created by the cylinder is twice as high as in the first instance, due to the presence of twice as many phosphate groups as in the first case.

The Poisson–Boltzmann theory assumes that the excess of bulk salt concentration around the molecule is an exponential function of the potential at the given point. A rough estimate of the difference in energy between the double stranded state and the separated strands gives

$$\Delta\Delta G(\phi) = \int_\Omega 2\phi e c^b (e^{2\phi} - e^{\phi})\, dx. \tag{23}$$

This is an increasing function of ϕ and, at high potentials (highly charged small molecules), the difference between the third terms of the energy-density integral (see Eq. (20)) will overshoot the difference between the electrostatic terms. In our examples, the fast increase of the interaction energies with the size of the system can be clearly seen in Table III.

These last considerations show the limits of application of the NLPBE while, as we have seen, the LPBE has its well-known shortcomings for high concentrations of bulk ions. A high ionic strength environment and/or systems with low charge density seem to provide the optimum conditions to apply the NLPBE as it has been pointed out in early works on the subject [3]. The key to achieving better accuracy is using methods of controllable precision like the simplified integral method, NLPBE2.

ACKNOWLEDGMENTS

The authors thank the NSF (award number ASC-9217374 which includes funds from DARPA) and the Robert A. Welch Foundation for partial support of this work. We thank Drs. Jim Briggs and Malcolm Davis for many technical discussions about UHBD. We thank our reviewers for useful suggestions.

REFERENCES

1. B. A. Luty, M. E. Davis, and J. A. McCammon, *J. Comput. Chem.* **9,** 1114 (1992).
2. E. S. Reiner and C. J. Radke, *J. Chem. Soc. Faraday Trans.* **86,** 3901 (1990).
3. K. A. Sharp and B. Hönig, *J. Phys. Chem.* **94,** 7684 (1990).
4. H.-X. Zhou, *J. Chem. Phys.* **100,** 3152 (1994).
5. C. L. Brooks III, Martin Karplus, and B. M. Pettitt, *Advances in Chemical Physics,* edited by I. Prigogine and S. A. Rice (Wiley, New York, 1988), Vol. LXXI.
6. M. E. Davis, J. D. Madura, B. A. Luty, and J. A. McCammon, *Comput. Phys. Commun.* **62,** 187 (1991).
7. J. D. Madura, J. M. Briggs, R. C. Wade, M. E. Davis, B. A. Luty, A. Ilin, J. Antosciewicz, M. K. Gilson, B. Bagheri, L. R. Scott, and J. A. McCammon, *Comput. Phys. Commun.* **91,** 57 (1995).
8. M. K. Gilson, M. E. Davis, B. A. Luty, and J. A. McCammon, *J. Phys. Chem.* **97,** 3591 (1993).
9. H. van Keulen and J. A. M. Smit, *J. Colloid Interface Sci.* **170,** 134 (1995).
10. E. Feitosa, A. A. Neto, and H. Chaimovich, *Langmuir* **9,** 702 (1993).
11. S. L. Carnie and D. Y. C. Chan, *J. Colloid Interface Sci.* **155,** 297 (1993).
12. S. L. Carnie, D. Y. C. Chan, and J. Stankovich, *J. Colloid Interface Sci.* **165,** 116 (1994).
13. K. E. Forsten, R. E. Kozack, D. A. Lauffenberger, and S. Subramanian, *J. Phys. Chem.* **98,** 5586 (1994).
14. Y. N. Vorobjev and H. A. Scheraga, *J. Phys. Chem.* **97,** 4855 (1993).
15. M. Schaefer and M. Karplus, *J. Phys. Chem.* **100,** 1578 (1996).
16. T. J. A. Ewing and T. P. Lybrand, *J. Phys. Chem.* **98,** 1748 (1994).
17. V. Vlachy and A. D. J. Haymet, *J. Chem. Phys.* **84,** 5874 (1986).
18. Y.-K, Cheng and B. M. Pettitt, *Prog. Biophys. Mol. Biol.* **58,** 225 (1992).
19. N. T. Thuong and C. Hélène, *Angew. Chem. Int. Engl.* **32,** 666 (1993).
20. E. Uhlmann and A. Peyman, *Chem. Rev.* **90,** 544 (1990).
21. S. C. Zimmerman and P. Schmitt, *J. Am. Chem. Soc.* **117,** 10769 (1995).
22. B-W. Zhou, E. Puga, J. S. Sun, T. Garestier, and C. Hélène, *J. Am. Chem. Soc.* **117,** 10425 (1995).
23. C. Hélène and J. J. Toulmé, *Oligodeoxynucleotides: Antisense Inhibitors of Gene Expression,* edited by J. S. Cohen (McMillan, London, 1989), p. 137.
24. D. S. Pilch, R. Brousseau, and R. H. Shafer, *Nucl. Ac. Res.* **18,** 5743 (1990).
25. S. Brenner and L. R. Scott, *The Mathematical Theory of Finite Element Methods* (Springer-Verlag, New York/Berlin, 1994).
26. D. McQuarrie, *Statistical Mechanics* (Harper & Row, New York, 1976).
27. M. Gilson, K. A. Sharp, and B. Hönig, *J. Comput. Chem.* **9,** 327 (1988).
28. M. Zacharias, B. A. Luty, M. E. Davis, and J. A. McCammon, *Biophys. J.* **63,** 1280 (1992).
29. V. Mohan, M. E. Davis, J. A. McCammon, and B. M. Pettitt, *J. Am. Chem. Soc.* **96,** 6428 (1992).
30. A. H. Elcock and J. A. McCammon, *J. Am. Chem. Soc.* **117,** 10161 (1995).
31. S. Arnott, R. Chandrasekeharan, D. L. Birdsall, A. G. W. Leslie, and R. L. Ratliffe, *Nature* **283,** 743 (1980).
32. *QUANTA, Version* 4.1 (Molecular Simulations Inc., 200 Fifth Avenue, Waltham, MA, 1994).
33. M. E. Davis and J. A. McCammon, *J. Comput. Chem.* **12,** 909 (1991).
34. B. Hönig and A. Nicholls, *Science* **268,** 1144 (1995).
35. R. H. Fowler, *Statistical Mechanics* (Cambridge Univ. Press, Cambridge, UK, 1929).
36. L. Onsager, *Chem. Rev.* **13,** 73 (1933).
37. J. G. Kirkwood, *J. Chem. Phys.* **2,** 767 (1934).
38. J. O. Bockris and A. K. N. Reddy, *Modern Electrochemistry* (Plenum, New York, 1970).